Applied Microscopy
Korean Society of Microscopy

pISSN 2287-5123 · eISSN 2287-4445
https://doi.org/10.9729/AM.2017.47.3.121

Regular Article

Investigations of Temperature Effect on the Conduction Mechanism of Electrical Conductivity of Copolymer/Carbon Black Composite

M. El Hasnaoui*, L. Kreit, L. C. Costa[1], M. E. Achour

LASTID Laboratory, Physics Department, Faculty of Sciences, Ibn-Tofail University, Kenitra 14000, Morocco
[1]I3N and Physics Department, University of Aveiro, Aveiro 3810-193, Portugal

*Correspondence to:
El Hasnaoui M,
Tel: +212-5-37-32-94-00
Fax: +212-5-37-32-94-33
E-mail: med.elhasnaoui@uit.ac.ma

Received July 30, 2017
Revised August 11, 2017
Accepted August 11, 2017

This study deals the prediction of temperature effect on low-frequency dispersion of alternating current (AC) conductivity spectra of composite materials based on copolymer reinforced with carbon black (CB) particles. A sample of ethylene butylacrylate loaded with 13% of CB particles were prepared and investigated using the impedance spectroscopy representation in the frequency range from 40 Hz to 0.1 MHz and temperature range from 20°C to 125°C. The dielectric constant, ε', and dielectric losses, ε'', were found to decrease with increasing frequency. The frequency dependence of the AC conductivity follows the universal power law with a large deviation in the high frequency region, the positive temperature coefficient in resistivity effect has been observed below the melting temperature which makes this composite potentially remarkable for industrial applications.

Key Words: Copolymer composite, Carbon black, Jonscher's power law, Permittivity, Positive temperature coefficient of resistivity effect

INTRODUCTION

It is known that the addition of conducting charges to polymers allows the modification of polymers' physical properties, as well as the implementation of new features in the polymer host matrix (Blom et al., 1998; Bouknaitir et al., 2017; He et al., 2016). The investigation of dielectric properties as a function of frequency and temperature is one of the most convenient methods of studying the transport mechanisms of polymer nanocomposite (El Hasnaoui et al., 2014). The polarization of a dielectric material composite is contributed by electronic, ionic, and dipolar polarization. It is proven that the dipole polarization requires relatively longer period of time than that of electronic and ionic polarization (Kimura & Kajiwara, 1998). For polar molecules, the dielectric constant decreases with frequency because the permanent dipoles cannot be reoriented quite quickly (Nigrawal & Chand, 2013). The understanding of conducting filler's effect on conduction mechanisms of polymers is still a work in progress.

The main interest of this study was to investigate the dielectric and electrical conductivity behaviours of ethylene butylacrylate (EBA) copolymer charged with 13% of carbon black (CB) nanopatricles and to their modeling. The relaxation parameters exhibited by the sample in the range from 40 Hz to 0.1 MHz was analyzed as a function of the temperature below and above the melting point.

MATERIALS AND METHODS

Sample of an EBA copolymer filled with 13% of acetylene CB used in this investigation were obtained from Borealis AB (Sweden). The butylacrylate monomer contains butylester side groups, providing a certain polarity and a relative low crystallinity (20%). The average size of the CB nanoparticles is about 30 nm (Mdarhri et al., 2007). For electrical measurements, the sample was prepared as disc

with a thickness of about 1 mm. Aluminium electrodes from 7 to 10 mm diameter were deposited on the opposite sides of the sample. The electrical leads were fixed by silver paint. Cross checking experiments were made, using different size electrodes.

During the electric measurements, the samples were maintained in a helium atmosphere in order to improve the heat transfer and eliminate the moisture. The impedance spectroscopy measurements were made from 40 Hz to 0.1 MHz and temperature range from 20°C to 125°C, using an Agilent 4294A precision impedance analyzer in the C_p-R_p configuration. The complex admittance $Y^*(\omega)=1/Z^*(\omega)=G(\omega)+jB(\omega)$ could be converted into complex permittivity formalism $\varepsilon^*=\varepsilon'-j\varepsilon''$ using the relations $\varepsilon'(\omega)=B(\omega)e/\varepsilon_0 A\omega$ and $\varepsilon''(\omega)=G(\omega)e/\varepsilon_0 A\omega$, where A is the cross-sectional area of the sample, e is its thickness and ε_0 is the free space permittivity. The terms $G(\omega)$ and $B(\omega)$ are respectively the conductance and the susceptance of the samples. Estimating relative errors on both real and imaginary part of the complex permittivity are $\Delta\varepsilon'/\varepsilon'=\Delta\varepsilon''/\varepsilon'<5\%$.

Differential scanning calorimetry (DSC) measurement was performed on a Shimatzu DSC-50 system, with a heating rate of 10°C/min from 20°C to 200°C. The sample is placed in a platinum cell with a lid and the reference cell is empty.

RESULTS AND DISCUSSION

DSC Analysis

The heating DSC thermogram of our sample is shown in Fig. 1. It is clear that an endothermic peak has been observed at about 90°C, which can be attributed to disordering in structure associated to the melting transition temperature, T_m. This spectrum reveals that this composite does not offer any exothermic change until 200°C.

Dielectric Analysis

The complex dielectric permittivity $\varepsilon^*=\varepsilon'-j\varepsilon''$ is a crucial parameter required in the design of electronic devices. The real part $\varepsilon'(\omega)$ is the dielectric constant which is related to the energy stored in the material, and imaginary part $\varepsilon''(\omega)$ is the dielectric loss which is proportional to the energy dissipated in each cycle of the electric field (Aziz & Abidin, 2014). The dielectric properties of this composite have been analyzed in terms of frequency and temperature. Fig. 2 shows the variation of dielectric loss, ε'', and dielectric constant, ε', as a function of frequency at various temperatures. It is observed that the ε' and ε'' continuously decrease with increasing frequency, whereas they show a decrease (below T_m) and increase (above T_m) at fixed frequency. The decrease of ε' with frequency could be attributed to the fact that at low frequencies ε', for polar materials, is due to the contribution of deformational polarization. When the frequency is increased, the dipoles cannot be able to rotate sufficiently rapidly, so that their oscillations lag behind those of the field. At high frequency, the dipoles will be unable to follow the field and the orientation polarization stopped, so ε' decreases, approaching a constant value due to the interfacial polarization (El-Nahass

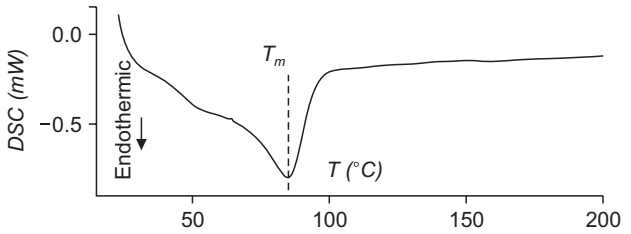

Fig. 1. Temperature dependence of the differential scanning calorimetry (DSC) signal for ethylene butylacrylate loaded with 13% of carbon black composite.

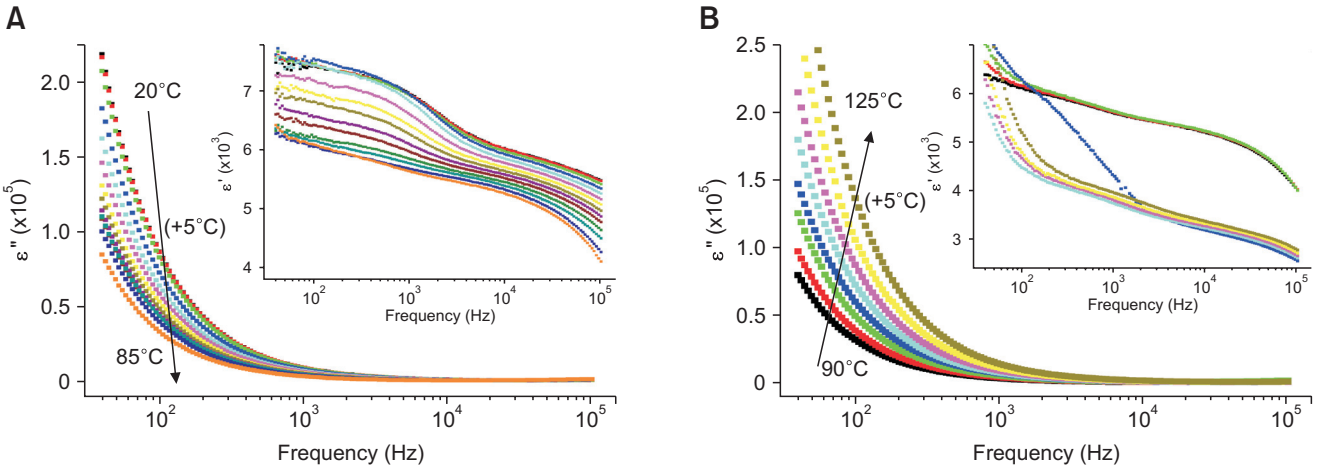

Fig. 2. Imaginary and real (inserted figure) parts of the effective complex permittivity of ethylene butylacrylate/carbon black composites versus frequency: for $T<T_m$ (A) and for $T>T_m$ (B).

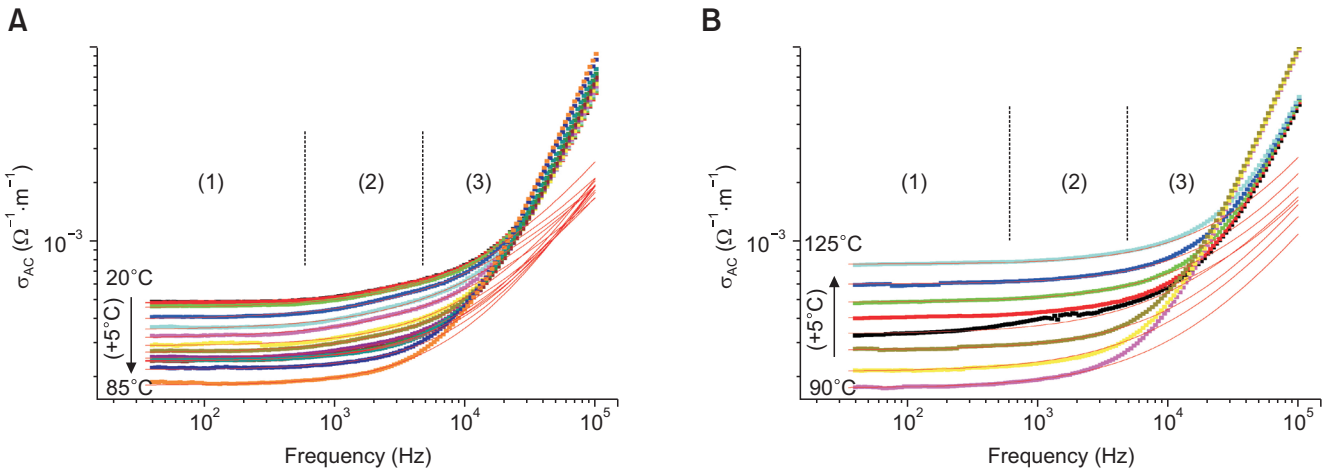

Fig. 3. Alternating current electrical conductivity of ethylene butylacrylate/carbon black composite versus frequency: for $T<T_m$ (A) and for $T>T_m$ (B). Symbols are data, and lines are the fitting results using the Jonscher's power law Eq. (2).

et al., 2016).

Electrical Conductivity Analysis

It has been demonstrated that the electrical conductivity provides significant information related to kinetic mechanisms of electronic charge carriers. The electrical conductivity $\sigma_{AC}(\omega,T)$ of the sample was calculated from dielectric losses, using the expression (Abazine et al., 2016):

$$\sigma_{AC}(\omega)=\omega\varepsilon_0\varepsilon''(\omega) \quad (1)$$

Fig. 3 shows the frequency dependent conductivity, below the melting point (Fig. 3A) and above of it (Fig. 3B). Three broad regions may be identified. At low frequencies ($F<F_{c1}$), the conductivity is almost constant behaviour corresponds to the direct current (DC) conductivity (Jonscher, 1983). It is observed in Table 1, that conductivity increases with temperature (for $T>T_m$) which is a feature of a thermally induced process due to the increase of the charge carrier energy (Costa et al., 2011). At intermediate frequency ($F_{c1}<F<F_{c2}$), the conductivity is frequency dependent. It is characterized by the universal Jonscher's power law of electrical conductivity (Kilbride et al., 2002; Xu et al., 2008):

$$\sigma_{tot}=\sigma_{DC}\left(1+p\left(\frac{\omega}{\omega_c}\right)^{s(T)}\right) \quad (2)$$

where σ_{DC} is the DC conductivity and is related to the drift mobility of the charge carriers, $s(T)$ is a frequency exponent parameter in the range $0<s<1$ characterizing the deviation from Debye behaviour. It represents the degree of interaction between the conducting charges and the macromolecular chains of the polymeric matrix, having a value of 0 for pure resistive behaviour and 1 for pure capacitive behaviour

Table 1. Electrical and dielectric parameters versus temperature obtained using the Jonscher's power law (Eq. 2)

T (°C)	σ_{DC} ($10^{-4}\Omega^{-1}$·m^{-1})	p	F_c (Hz)	s	R^2
20	4.79	0.09	1,241	0.89	0.996
25	4.76	0.08	1,068	0.86	0.996
30	4.51	0.11	1,066	0.77	0.997
35	3.94	0.11	738	0.72	0.996
40	3.47	0.12	804	0.75	0.995
45	3.15	0.11	678	0.72	0.996
50	2.88	0.06	625	0.89	0.997
55	2.65	0.08	651	0.82	0.995
60	2.48	0.08	792	0.91	0.993
65	2.39	0.07	732	0.92	0.998
70	2.41	0.08	1,015	1	0.996
75	2.41	0.07	1,055	1	0.996
80	2.17	0.07	962	1	0.999
85	1.81	0.1	1,016	1	0.995
90	1.75	0.1	800	0.93	0.993
95	2.13	0.1	935	0.82	0.995
100	2.74	0.09	1,001	0.81	0.989
105	3.32	0.11	1,100	0.8	0.956
110	4.01	0.08	1,262	0.83	0.998
115	4.83	0.08	1,479	0.85	0.991
120	5.99	0.06	1,600	0.92	0.999
125	7.57	0.06	1,800	0.91	0.998

R^2 represents the correlation coefficient.

(Ouewsleti et al., 2010). The constant p is dependent on the type of pair approximation in the network. The crossover frequency ω_c is a frequency ($\omega_c=2\pi F_{c1}$) at which the individual (parallel) pair processes percolate and that cause the appearance of series processes. The series processes in the low frequency range are non local and can be treated as percolation of individual particles over macroscopic distances in clusters or chains. The solid lines in Fig. 3 are obtained

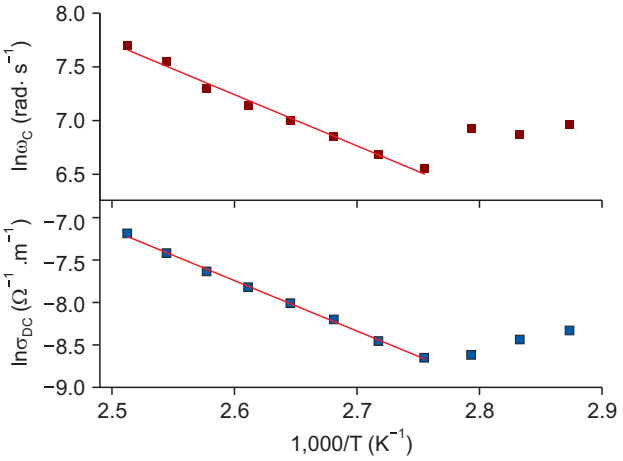

Fig. 4. Arrhenius plots of direct current (DC) electrical conductivity and crossover frequency versus the inverse of temperature. The solid lines represent the best linear fits of the experimental data.

from the fit of the Eq. (2). The obtained values of relaxation parameters are given in Table 1. As can be seen, the values of frequency exponent *s* are in the range 0.80~0.92 for the temperature above the melting point and are temperature independent. There are a several number of theoretical approaches to deduce this behaviour from the microscopic transport properties of various classes of materials (Elliot, 1987). The quantum-mechanical tunnelling model, which corresponds to the variable range hopping model for nonzero frequencies, predicts a temperature-independent frequency exponent *n* near 0.8 (Elliot, 1987). In other work (Dyre, 1988); It has been shown that an approximate universal power law with an exponent value in the range 0.8~1.0 is characteristic of hopping in disordered composite material where hopping charge carriers are subject to spatially randomly varying energy barriers. This agrees with the fluctuation induced tunnelling model. The DC conductivity and the crossover frequency ω_c are temperature dependent, and this behaviour will be discussed after. At high frequencies, the conductivity has a dispersion that shifts to higher frequencies, a third domain emerged towards up to the second crossover frequency (F_{c2}>5 kHz) which is probably the beginning of the transition to another electrical behaviour that characterise the response of conductivity at high frequencies (Mohamed et al., 2001).

From Table 1, the DC conductivity and the crossover frequency ω_c increase with temperature, for the temperatures above the melting point. This behaviour was modelled using the thermal Arrhenius relations (Rim et al., 2006; Song et al., 2007): $\sigma_{DC} \propto \exp(E_{DC}/k_bT)$ and $\omega_c \propto \exp(E_{AC}/k_bT)$ where k_b is the Boltzmann's constant, E_{DC} and E_{AC} represent the activation energies obtained respectively from the DC and alternating current (AC) conductivities. Fig. 4 displays the representations of σ_{DC} and ω_c versus the inverse of temperature. The straight line in Fig. 4, shows an activated thermal behaviour for temperature above T_m, the calculated values of activation energies are E_{DC}=(0.41±0.02) eV and E_{AC}=(0.51±0.01) eV, smaller than those obtained using composite material based on CB loaded in epoxy resin matrix (Macutkevic et al., 2013). The difference may be related to the type of the matrix that has been used in each composite because the polyester and epoxy resin matrices do not have the same thermal and mechanical properties.

CONCLUSIONS

The effective complex permittivity and the electrical conductivity of EBA loaded with 13% of CB particles was studied over a frequency range from 40 Hz to 100 kHz and in a temperature range from 20°C to 125°C by impedance spectroscopy. This study exhibits typical dielectric changes process and a specific behavior versus frequency which was modelled using the Jonscher's power law. The activation energies obtained from DC and AC conductivities showed a weak interaction between carbon filler and the macromolecular network.

CONFLICT OF INTEREST

No potential conflict of interest relevant to this article was reported.

ACKNOWLEDGMENTS

This works is partially supported by Morocco-Portugal cooperation program (No. Physique 04/08/9).

REFERENCES

Abazine K, Anakiou H, El Hasnaoui M, Grac M P F, Fonseca M A, Costa L C, Achour M E, and Oueriagli A (2016) Electrical conductivity of multiwalled carbon nanotubes/polyester polymer nanocomposite. *J. Compos. Mater.* **50**, 3283-3290.

Aziz S B and Abidin Z H Z (2014) Electrical and morphological analysis of chitosan: AgTf solid electrolyte. *Mater. Chem. Phys.* **144**, 280-286.

Blom P W M, Schoo H F M, and Matters M (1998) Electrical characterization of electroluminescent polymer/nanoparticles composite devices. *Appl. Phys. Lett.* **73**, 3914-3916.

Bouknaitir I, Aribou N, Elhad Kassim S A, El Hasnaoui M, Melo B M

G, Achour M E, and Costa L C (2017) Electrical properties of conducting polymer composites: Experimental and modeling approaches. *Spectro. Lett.* **50**, 196-199.

Costa M M, Pires G F M, Terezo A J, Graca M P F, and Sombra A S B (2011) Impedance and modulus studies of magnetic ceramic oxide Ba2Co2Fe12O22 (Co2Y) doped with Bi2O3. *J. Appl. Phys*. **110**, 034107.

Dyre J C (1988) The random free energy barrier model for ac conduction in disordered solids. *J. Appl. Phys*. **64**, 2456-2468.

El Hasnaoui M, Triki A, Achour M E, and Arous M (2014) Modelling of dielectric relaxation processes of epoxy-resin filled with carbon black particles. *Physica B* **433**, 62-66.

Elliot S R (1987) Ac conduction in amorphous chalcogenide and pnictide semiconductors. *J. Adv. Phys.* **36**, 135-217.

El-Nahass M M, Farid A M, and Atta A A (2016). AC conductivity and dielectric relaxation of bulk tris. (8-hydroxyquinoline) aluminum organic semiconductor. *Opt. Quant. Electron.* **48**, 458.

He D, Li Y, Wang J, Yang Y, and An Q (2016) Tunable nanostructure of TiO2/reduced graphene oxide composite for high photocatalysis. *Appl. Microsc.* **46**, 37-44.

Jonscher A K (1983) *Dielectric Relaxation in Solids* (Chelsea Dielectrics Press, London).

Kilbride B E, Coleman J N, Fraysse J, Fournet P, Cadek M, Drury A, Hutzler S, Roth S, and Blau W J (2002) Experimental observation of scaling laws for alternating current and direct current conductivity in polymer-carbon nanotube composite thin films. *J. Appl. Phys.* **92**, 4024-4030.

Kimura T and Kajiwara M (1998) Electrical properties of poly(n-butylamino) (di-allylamino) phosphazene. *J. Mater. Sci.* **33**, 2955-2959.

Macutkevic J, Kuzhir P, Paddubskaya A, Makimono S, Banys J, Celzard A, Fierro V, Bistarelli S, Cataldo A, Micciulla F, and Bellucci S (2013) Electrical transport in carbon black-epoxy resin composites at different temperatures. *J. Appl. Phys.* **114**, 033707.

Mdarhri A, Brosseau C, and Carmona F (2007) Microwave dielectric properties of carbon black filled polymers under uniaxial tension. *J. Appl. Phys.* **101**, 084111.

Mohamed A, Miane J L, and Zangar H (2001) Radiofrequency and microwave (10kHz–8GHz) electrical properties of polypyrrole and polypyrrole-poly(methyl methacrylate) composites. *Polym. Int.* **50**, 773–777.

Nigrawal A and Chand N (2013) Electrical and dynamic mechanical analysis of nano alumina addition on polyvinyl alcohol (Pva) composites. *Prog. Nanotechnol. Nanomater.* **2**, 25-33.

Ouewsleti A, Hilel F, Guidara K, and Gargouri M (2010) AC conductivity analysis and dielectric relaxation behavior of $[N(C_3H_7)_4]_2Cu_2Cl_6$. *J. Alloys Compd.* **49**, 508-514.

Rim Y H, Lee B S, Choi H W, Cho J H, and Yang Y S (2006) Electrical relaxation of bismuth germanate silicate glasses. *J. Phys. Chem. B* **110**, 8094-8099.

Song C H, Choi H W, Kim M, Jin G Y, and Yang Y S (2007) Electrical Relaxations of Amorphous xKNbO-3 (1-x) SiO-2 (x=0.33, 0.5, 0.67, 0.8). *J. Korean Phys. Soc.* **51**, 674-677.

Xu H, Zhang S, Anlage S M, Hu L, and Grüner G (2008) Frequency- and electric-field-dependent conductivity of single-walled carbon nanotube networks of varying density. *Phys. Rev. B* **77**, 075418.